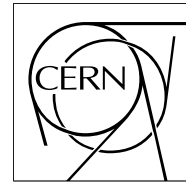**The Compact Muon Solenoid Experiment**

CMS Note

Mailing address: CMS CERN, CH-1211 GENEVA 23, Switzerland

20 January 2006

Systematic uncertainties of the top background in the $H \rightarrow WW$ channel

G. Davatz,

Institute for Particle Physics, ETH Zürich, Switzerland

A.-S. Giolo-Nicollerat,

CERN, Geneva, Switzerland

M. Zanetti

Dipartimento di Fisica 'Galileo Galilei', Universitá di Padova, Italy

Abstract

The $t\bar{t}$ process is one of the main backgrounds in the search for the Higgs boson in the $H \rightarrow WW \rightarrow \ell\nu\ell\nu$ channel. The simulation of this background as well as an estimation of its contribution to the total systematic uncertainty of this search will be studied in detail. The predictions of the PYTHIA, HERWIG, TopREX and MC@NLO Monte Carlo programs are compared in order to estimate the effect of different showering programs and of spin correlations. Furthermore, the question of how to include NLO corrections is addressed and the simulation of single top background at NLO discussed. Different data-driven methods to normalize the $t\bar{t}$ background are proposed and compared, and their experimental uncertainties are estimated using a full CMS simulation.

1 Introduction

The Higgs-boson decay into two W bosons and subsequently into two leptons ($H \rightarrow WW \rightarrow \ell\nu\ell\nu$) is expected to be the main discovery channel for intermediate Higgs-boson masses: between $2m_W$ and $2m_Z$ [1]. The signature of this decay is characterized by two leptons and high missing energy. In this mass range, the $H \rightarrow WW$ branching ratio is close to one, leading to high statistics.

However, since no narrow mass peak can be reconstructed in this channel, a good background control together with a high signal to background ratio is needed. The most important backgrounds, which give a signature similar to the signal (i.e. two leptons and missing energy) are continuum WW production and $t\bar{t}$ production. To reduce these backgrounds, one has to require a small opening angle between the leptons in the plane transverse to the beam and apply a jet veto.

In this note, $t\bar{t}$ production is studied in detail and its contribution to the total systematic uncertainties on the background determination in the $H \rightarrow WW \rightarrow \ell\nu\ell\nu$ search is estimated.

In the first part of this note, the generation of $t\bar{t}$ background will be studied by comparing different Monte Carlo generators. The issue of a good simulation of this process at Next to Leading Order (NLO) will be addressed together with the effect of spin correlations. Then the inclusion of single resonant top production at Next to Leading Order will be discussed. Finally, methods to normalize the top background using data will be studied. Experimental uncertainties coming from different normalization procedures will be estimated using a full CMS simulation.

2 Generation of $t\bar{t}$ events

In this section the generation of top production ($pp \rightarrow t\bar{t} \rightarrow WbW\bar{b} \rightarrow \ell\nu\ell\nu b\bar{b}$, with ℓ = e, μ and τ) will be discussed by comparing four different Monte Carlo generators: PYTHIA [2], TopReX [3], HERWIG [4] and MC@NLO [5], whose characteristics are summarized in Table 1.

HERWIG and PYTHIA are Monte Carlo generators based on Leading Order (LO) matrix elements. Additional jet activity is generated through the so-called parton shower. The parton shower accurately describes soft and collinear emissions. It tends however to underestimate the hard emissions. HERWIG is based on the Cluster model for hadronization, whereas PYTHIA uses the Lund hadronization model.
TopREX is a Monte Carlo based on LO matrix elements, relying on PYTHIA for the showering process. Exact LO matrix elements for 2→n (n up to 6) processes are taken into account and spin correlations are consistently propagated through the generated processes.
MC@NLO, on the other hand, combines exact Next to Leading Order (NLO) computation with parton shower Monte Carlo generators. It is based on HERWIG for the hadronization step. Therefore hard emissions are treated as in NLO computations, whereas soft and collinear emissions are treated as in a LO parton shower Monte Carlo program. The matching between the hard and soft and collinear regions is smooth. The total rates in MC@NLO are accurate to NLO.
No spin correlations between the t and $\bar{t}$ are taken into account in PYTHIA and MC@NLO, while HERWIG and TopReX have the option to include them.

Table 1: Comparison of the different Monte Carlo generators.

	PYTHIA 6.227	TopREX 4.11	HERWIG 6.508	MC@NLO 2.31
Matrix Elements	LO	LO	LO	NLO
hadronization model	LUND	LUND	Cluster	Cluster
shower model	Q^2 ordered	Q^2 ordered	angular ordered	angular ordered
spin correlations between t and $\bar{t}$	no	yes	yes	no

In the following, three points will be addressed: how well LO Monte Carlos generate top production in the phase space relevant for the Higgs-boson search with respect to NLO Monte Carlos, whether different showering models used by PYTHIA and HERWIG imply differences in the shapes of some important variables, whether spin correlations need to be taken into account.

For the first point, MC@NLO will be compared with HERWIG without spin correlation, in order to study the NLO effect separately. Then, PYTHIA and HERWIG without spin correlation will be compared to study the different showering models. The third question will be addressed with a comparison between HERWIG with and without spin correlation and MC@NLO on one hand and TopReX with and without spin correlation and PYTHIA on the

other hand.

For the first part of this study, cuts based on the CMS geometrical acceptance were applied on the generated 4-vectors. The PDF chosen for HERWIG, PYTHIA and TopReX is CTEQ5L while CTEQ5M1 is used for MC@NLO. No underlying event was generated. The top-quark mass considered is 175 GeV. One million events were generated with each generator.
The cross section of $pp \to t\bar{t}$ is 514 pb in PYTHIA, 400 pb in HERWIG and 837 pb in MC@NLO. The factorization scale μ_{fac} and renormalization scale μ_{ren} chosen for MC@NLO are equal to $m_{top}/2$. For PYTHIA and HERWIG, default scales are used. The difference between the cross section in PYTHIA and HERWIG is expected to be mostly due to this different default scale choice. The default scales were chosen as this is how the Monte Carlo samples in CMS are currently produced. All different Monte Carlo cross sections will be reweighted to the the inclusive NLO cross section, 840 pb.

Getting an accurate NLO simulation

Up until recently only Monte Carlo generators based on LO matrix elements were available for the simulation of $t\bar{t}$ processes and used for most CMS Monte Carlo samples. In order to get an accurate cross section including higher order QCD corrections, the cross section of the simulated process can be normalized to the calculated NLO cross section applying a so-called inclusive K-factor, which is just the ratio of the NLO cross section over the LO cross section.

Such an approximation assumes that all the dynamics is the same in both LO and NLO. Otherwise, one would have to consider for instance p_t-dependent or rapidity-dependent K-factors in order to match generators based on LO and parton shower with generators at NLO[1].

To estimate the accuracy of the use of constant K-factors with LO Monte Carlos for the $t\bar{t}$ simulation, HERWIG 6.508 without spin correlation and MC@NLO 2.31 linked to this HERWIG version were compared. HERWIG 6.508 is an update of HERWIG 6.507 version[2]. As the spin correlations are not included in any of these simulations (this option is not yet available in MC@NLO) and the same showering model is used, the difference between the two simulations should be mostly due to the additional NLO matrix elements in MC@NLO.
This question is particularly interesting in the case of the Higgs-boson search in the WW channel, since a jet veto has to be applied, making the event selection more sensitive to the jet content of the different processes.

One million $pp \to t\bar{t} \to WbW\bar{b} \to \ell\nu\ell\nu b\bar{b}$ events were generated and the events for this comparison were reconstructed starting with stable particles from the generator tree.

The selection used to search for the $H \to WW$ signal was then applied. First, a preselection requires two isolated [3] opposite charged leptons with E_t larger than 20 GeV and $|\eta|$ lower than 2 and rejecting all events including a jet[4] with E_t larger than 30 GeV and $|\eta| < 2.5$ (jet veto). The second part of the selection requires:

- $E_t^{miss} > 40$ GeV (E_t^{miss} is formed with the sum of isolated leptons and jets transverse momenta)

- $\phi_{\ell\ell} < 45°$ (angle between the leptons in the transverse plane)

- 5 GeV $< m_{\ell\ell} < 40$ GeV (the invariant mass of the two leptons)

- 30 GeV $< p_t^{\ell\,max} < 55$ GeV (lepton with the largest p_t)

- $p_t^{\ell\,min} > 25$ GeV (lepton with the smallest p_t)

---

[1] For instance, p_t- and efficiency- dependent K-factors are defined to get a more accurate simulation of $H \to WW$ [6].

[2] The directions of the top decay products in HERWIG 6.507, particularly the b quark, were shifted too much by the parton showering.

[3] The isolation variable was defined as the ratio of the energy sum of all stable particles inside a narrow cone around the lepton ($\Delta R=0.15$) over the energy sum of all stable particles inside a larger cone ($\Delta R=0.5$). The isolation variable has then to be larger than 0.9. To be taken into the energy sum, the transverse momentum of a particle has to be larger than 1 GeV. The p_t of an isolated lepton should be larger than 10 GeV.

[4] The jets are reconstructed using an Iterative Cone Algorithm with a Cone Size, ΔR, of 0.5. A jet is kept if its p_t is larger than 20 GeV and $|\eta| < 4.5$.
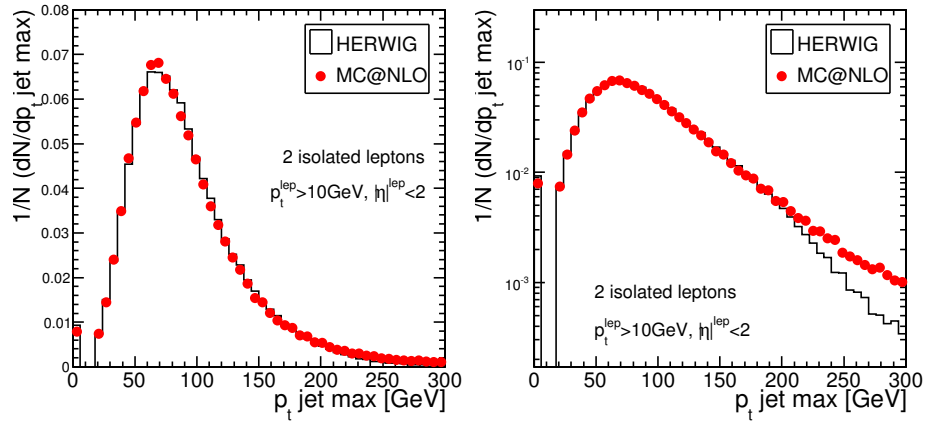
Figure 1: The p_t distribution of the leading jet in HERWIG and MC@NLO in linear and logarithmic scale.
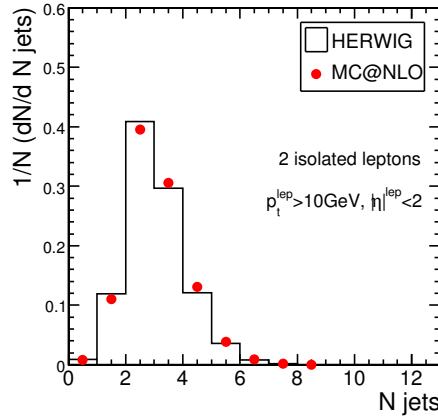

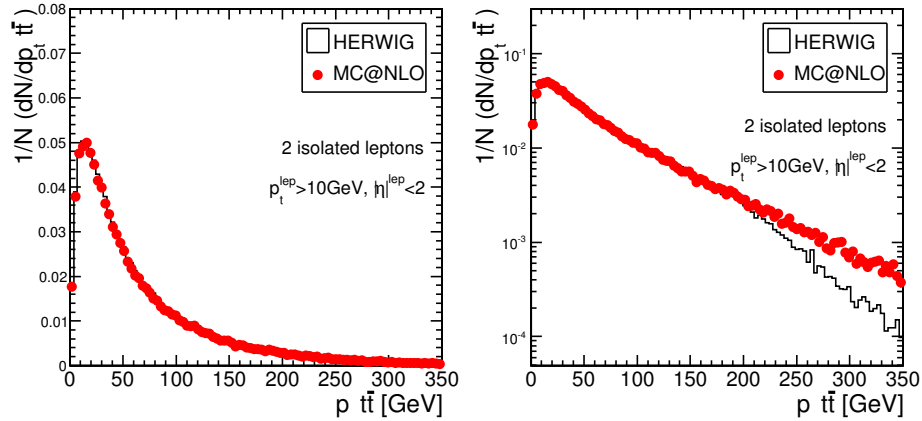Figure 2: The number of jets in HERWIG and MC@NLO.

Figure 3: The p_t distribution of the $t\bar{t}$ system in HERWIG and MC@NLO in linear and logarithmic scale.

Figure 1 shows the transverse momentum of the leading jet for HERWIG and MC@NLO. The shapes look very similar, except in the high p_t region. MC@NLO produces harder jets than HERWIG. This is not surprising since HERWIG, as a LO parton shower Monte Carlo generator, produces jets rather correctly in the soft and collinear region, but is inaccurate in the high p_t region. As a jet veto is applied in the selection cuts, the two Monte Carlo generators are very similar in our region of interest. Figure 2 shows that HERWIG and MC@NLO produce about the same number of jets. Figure 3 shows the transverse momentum of the $t\bar{t}$ system in HERWIG and MC@NLO. The $p_{t\ jet\ max}$ and $p_{t\ \bar{t}}$ variables are strongly correlated, as the $t\bar{t}$ system is balanced by jets.

Again, the transverse momentum spectrum is harder in MC@NLO, but HERWIG and MC@NLO agree very well at low p_t.

Table 2 shows the number of events and the relative selection efficiencies[5] for HERWIG and MC@NLO. In order to investigate the NLO contribution, one has to compare only the first four columns, corresponding to MC@NLO and HERWIG without spin correlations. One would expect differences mostly in the jet veto efficiency and the isolation: these differences are actually very small. The relative efficiency of the jet veto in MC@NLO is 0.029 while in HERWIG its 0.032. As there are already two b-jets in the $t\bar{t}$ final state, the jet veto will tend to be less sensitive to additional jet activity. In addition the shapes of all the other cut variables are very similar in MC@NLO and HERWIG without spin correlation.

This comparison shows that the NLO contribution has a small effect on the shapes of the variables considered and the selection efficiencies for the phase space relevant for the $H \rightarrow WW$ search. The region where NLO makes a difference is at very high p_t, whereas the bulk of the selected events is in the low p_t region. It should therefore be safe to use an inclusive K-factor to get from HERWIG to MC@NLO.

Table 2: Number of events after selection cuts for MC@NLO and HERWIG with and without spin correlation. The relative efficiency is given after each specific cut is applied. One million events were generated with each Monte Carlo.

	MC@NLO 2.31 without spin correlations		HERWIG 6.508 without spin correlations		with spin correlations	
	nr of events	rel. eff.	nr of events	rel. eff.	nr of evts	rel. eff.
2 isol. leptons	280656	0.2807 ± 0.0004	284876	0.2849 ± 0.0004	288015	0.2880 ± 0.0004
$\|\eta^{\ell ep}\| < 2$	197614	0.7041 ± 0.0009	193553	0.6795 ± 0.0009	196034	0.6806 ± 0.0009
jet veto	5764	0.0292 ± 0.0004	6159	0.0318 ± 0.0004	6046	0.0308 ± 0.0004
$E_t^{miss} > 40$	4027	0.699 ± 0.006	4414	0.717 ± 0.006	4489	0.743 ± 0.006
$\phi_{\ell\ell} < 45°$	608	0.151 ± 0.006	632	0.143 ± 0.005	724	0.161 ± 0.006
5 GeV < $m_{\ell\ell} < 40$ GeV	354	0.58 ± 0.02	379	0.60 ± 0.02	416	0.57 ± 0.02
30 GeV< $p_t^{\ell\,max} < 55$ GeV	164	0.46 ± 0.02	194	0.51 ± 0.03	191	0.46 ± 0.02
$p_t^{\ell\,min} > 25$ GeV	71	0.43 ± 0.04	76	0.39 ± 0.04	77	0.40 ± 0.04

Effect of the showering model

The effects of different showering models on the variable shapes and selection efficiencies is studied by comparing PYTHIA 6.227, based on the Lund hadronization model, with HERWIG without spin correlations, based on the cluster hadronization model.

Figure 4 shows the number of jets and Figure 5 the p_t spectrum of the hardest jet for PYTHIA and HERWIG. On average, PYTHIA produces fewer and softer jets than HERWIG. The shape of the transverse momentum of the $t\bar{t}$ system is different in PYTHIA and HERWIG. HERWIG tends to be smaller in the lower p_t region whereas PYTHIA is larger in the higher p_t region, as shown in Figure 6. However, the shapes of the other selection variables show no large differences, as an example Figure 7 shows the maximum lepton transverse momentum before and after the selection cuts.

The third and forth column in Table 2 and the first and second column in Table 3 compare the relative efficiencies of PYTHIA and HERWIG without spin correlations. The isolation of the leptons is very similar between HERWIG and PYTHIA, however the jet veto leads to a higher acceptance of the $t\bar{t}$ background in PYTHIA with respect to HERWIG, as the jets are softer and therefore fewer events are rejected. The relative efficiency ϵ in HERWIG is 0.032 while in PYTHIA it's 0.037. This is about a difference of around 15 %.

This comparison shows that for the phase space relevant to the $H \rightarrow WW$ search, HERWIG and PYTHIA predict very similar variable shapes and relative selection efficiencies, except for the jets and the $t\bar{t}$ system. PYTHIA produces fewer and softer jets than HERWIG. The peak of the p_t spectrum is shifted to lower p_t than in HERWIG. The difference due to the showering model can therefore be mostly observed in the jet veto efficiency and is around 15 %.

This shows that the uncertainty due to different showering models is rather large, mostly due to the different

---

[5] Relative efficiency means here the ratio between the number of events after and before the cut is applied.
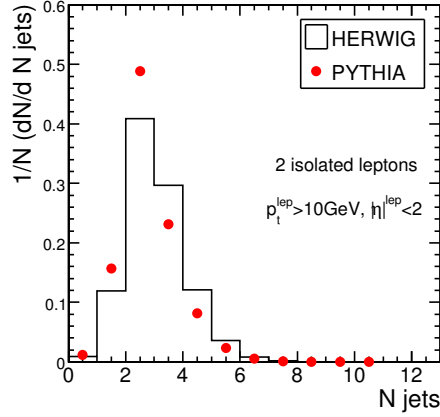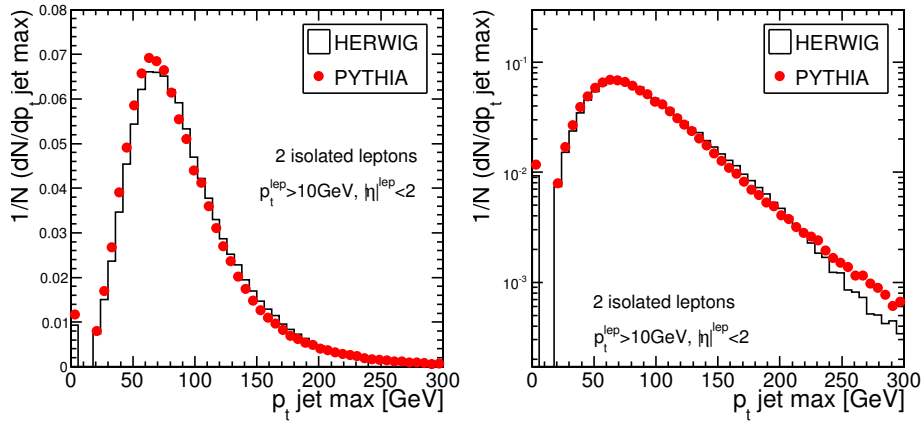
Figure 4: The number of jets in HERWIG and PYTHIA

Figure 5: The p_t distribution of the leading jet in HERWIG and PYTHIA in linear (left) and logarithmic scale (right).
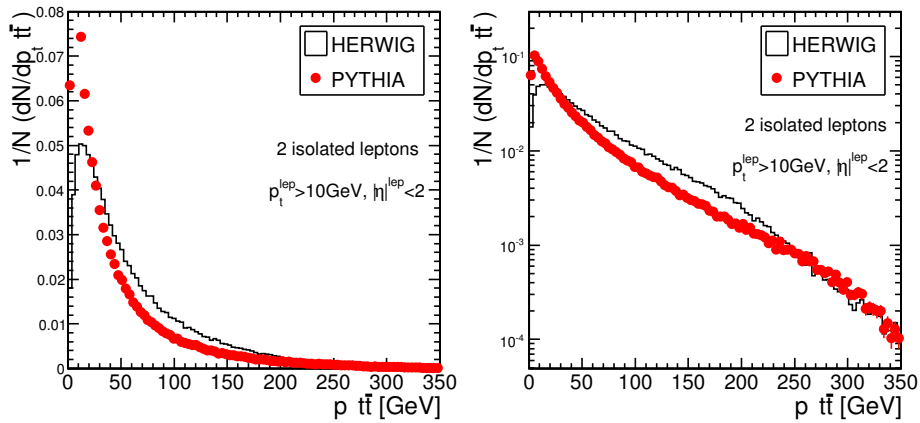

Figure 6: The p_t distribution of the $t\bar{t}$ system in HERWIG and PYTHIA in linear (left) and logarithmic scale (right).

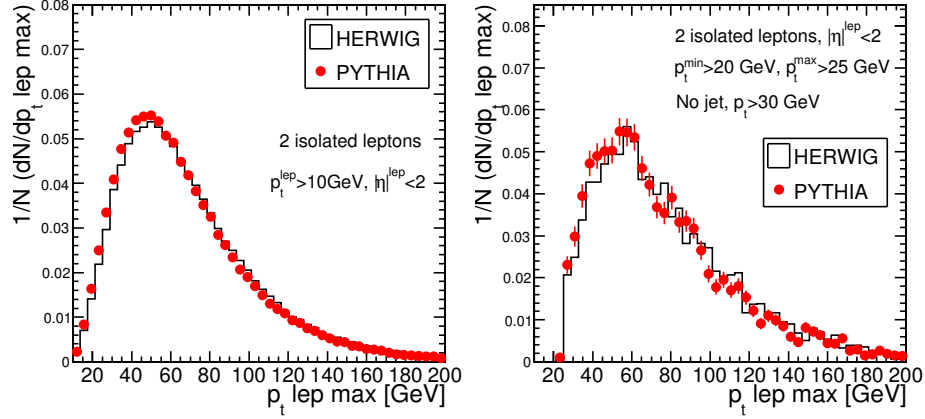treatment of jets, which can be observed in the $p_{t\bar{t}}$ spectrum.

Figure 7: The p_t distribution of the lepton with the highest p_t in HERWIG and PYTHIA before (left) and after (right) the main cuts are applied.

Table 3: Number of events after selection cuts for PYTHIA and TopReX with and without spin correlations. The relative efficiency is given after each specific cut is applied. One million events were generated with each Monte Carlo.

| | PYTHIA 6.227 | | TopReX | | | |
| | without spin correlations | | without spin correlations | | with spin correlations | |
	nr of events	rel. eff.	nr of events	rel. eff.	nr of evts	rel. eff.
2 isol. leptons	281624	0.2816 ± 0.0004	293670	0.2937 ± 0.0005	295707	0.2957 ± 0.0005
$|\eta^{\ell ep}| < 2$	195343	0.6936 ± 0.0009	203689	0.6936 ± 0.0009	205605	0.6953 ± 0.0009
jet veto	7128	0.0365 ± 0.0004	7804	0.0383 ± 0.0004	7834	0.0381 ± 0.0004
$E_t^{miss} > 40$	4976	0.698 ± 0.005	5442	0.697 ± 0.005	5586	0.713 ± 0.005
$\phi_{\ell\ell} < 45°$	731	0.147 ± 0.005	801	0.147 ± 0.005	962	0.172 ± 0.005
5 GeV < $m_{\ell\ell} < 40$ GeV	434	0.59 ± 0.02	499	0.62 ± 0.02	594	0.62 ± 0.02
30 GeV< $p_t^{\ell\,max} < 55$ GeV	214	0.49 ± 0.02	258	0.52 ± 0.02	296	0.50 ± 0.02
$p_t^{\ell\,min} > 25$ GeV	85	0.40 ± 0.03	113	0.44 ± 0.03	125	0.42 ± 0.03

Effect of the spin correlations

In the H $\rightarrow$ WW channel, a cut has to be applied on the opening angle between the leptons in the transverse plane, in order to differentiate the signal from WW continuum production. This makes the selection more sensitive to spin correlations. To study this, the TopReX Monte Carlo is used. It is interfaced to the PYTHIA for the showering step. TopReX with spin correlations is compared to PYTHIA and TopReX without spin correlations[6]. Then HERWIG with spin correlations is compared to HERWIG and MC@NLO without spin correlations.

Differences originating from the inclusion of spin correlations are seen in the mass of the dilepton system and in the $\phi_{\ell\ell}$ distribution. Figure 8 and 9 show the angle $\phi_{\ell\ell}$ between the leptons for the samples with and without spin correlations. In the left plots, the only requirement is to have two isolated leptons with $p_t > 10$ GeV and $|\eta| < 2$. In the right plots, an additional jet veto is applied. A similar but smaller effect is observed in the $m_{\ell\ell}$ distribution.

PYTHIA and TopReX without spin correlations (Figure 8) show the same $\phi_{\ell\ell}$ distribution. Also HERWIG without spin correlations has the same $\phi_{\ell\ell}$ distribution as MC@NLO (Figure 9). The difference in the distribution with and without spin correlations is slightly larger in the TopReX case than in the comparison with HERWIG. This is most probably due to the fact that TopReX does not the allow the top quarks to radiate gluons. In both comparisons one can see that the spin correlations make the $\phi_{\ell\ell}$ distribution flatter. After a jet veto is applied, the distributions with and without spin correlations look more similar.

The Higgs-boson selection criteria were applied on both samples and Table 2 and 3 show the results. The rel-

---

[6] The difference between PYTHIA and TopReX without spin correlation is mostly due to the fact that the top quarks are not allowed to radiate gluons in TopReX, and the different treatment of m_{top}.
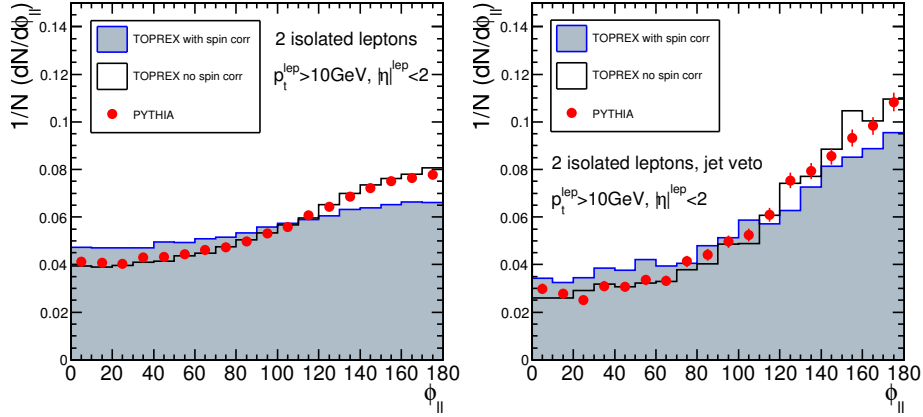
Figure 8: $\phi_{\ell\ell}$ distributions of the angle between the leptons in the plane transverse to the beam. TopReX with and without spin correlations is shown, as well as PYTHIA. On the left, only very basic cuts are applied, whereas on the right a jet veto is applied in addition. The Higgs-signal selection requires with $\phi_{\ell\ell} < 45°$.
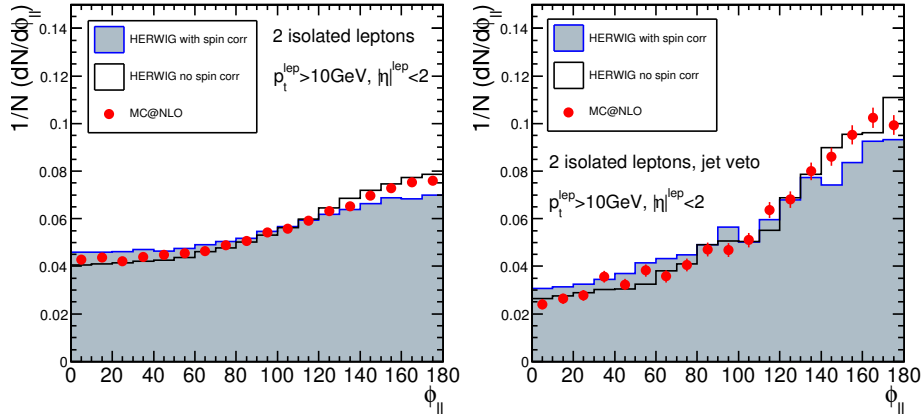

Figure 9: $\phi_{\ell\ell}$ distributions if the angle between the leptons in the plane transverse to the beam. HERWIG with and without spin correlations is shown, as well as MC@NLO. On the left, only very basic cuts are applied, whereas on the right a jet veto is applied in addition. The Higgs-signal selection requires $\phi_{\ell\ell} < 45°$.

ative efficiency after the $\phi_{\ell\ell}$ cut is 0.14 in HERWIG without spin correlations and 0.16 in HERWIG with spin correlations, while it's 0.15 in TopREX without spin correlations and 0.17 in TopREX with spin correlations. The relative efficiency in TopREX is slightly higher than in HERWIG. The difference of the relative efficiencies with and without spin correlations is about the same in both the TopReX and the HERWIG case.

In conclusion, the difference due to the spin correlations is around 10%. Moreover the difference due to the use of diverse showering models is around 15% between Herwig and Pythia and 20% between TopReX and Herwig.

These uncertainties cannot be neglected: it will be very important to estimate the $t\bar{t}$ background contribution for the Higgs-boson search using data. A method to do this will be presented in Section 4.

3   Generating single resonant top production

At leading order, the inclusive double-resonant top production process, $pp \rightarrow t\bar{t} \rightarrow WbWb \rightarrow \ell\nu\ell\nu bb$, where $\ell = e, \mu, \tau$, has a cross section times branching ratio of about 52 pb. Single resonant top production $pp \rightarrow Wt$ represents a contribution about ten times smaller. After applying a jet veto, the single-resonant top contribution is increased with respect to the double-resonant one, as the b-jet is produced at a much lower transverse momentum. This contribution therefore deserves particular care.

In order to resum large logarithms of the form $\log[(m_t + m_W)/m_b]$, it is preferable to view the single-resonant process as one in which a b quark is probed directly inside the proton. In this case, the single resonant leading order process is $gb \rightarrow Wt$, as depicted in Figure 10, right. Starting from this process one can calculate NLO corrections,

which naively include the double-resonant diagrams in the real radiation contribution [7]. However, by applying a veto on the presence of an extra b quark, the interference effect is greatly suppressed and the contribution from the double-resonant diagrams can be unambiguously removed [9].
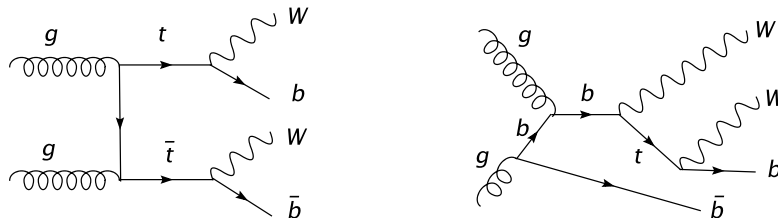

Figure 10: Examples of Feynman graphs for double-resonant (left) and single-resonant (right) top production

Therefore we can estimate the single- resonant top production rate at NLO in a region where a jet veto is applied, which in the case of the Higgs-boson search corresponds to the signal region. The NLO prediction for the rate depends on the region of phase space which is probed, in particular on the definition of the jet veto. In the following we will study the sensitivity to NLO corrections of the different kinematic variables used for $H \to WW \to \ell\nu\ell\nu$.

The NLO cross section for Wt production was calculated by J. Campbell and F. Tramontano using MCFM [10], a parton level Monte Carlo generator. The efficiencies obtained for the Higgs-boson selection cuts were compared for MCFM at LO and NLO by John Campbell and are shown in Table 4. The same selection as above is used. However since MCFM is a parton level generator, the jet veto had to be applied directly on the b-parton, requiring no b partons with $p_t > 40$ GeV. No requirement on the lepton isolation was added. If no selection is applied, the NLO-to-LO cross section ratio is about 1.4. After all selection cuts, it drops to 0.7, mostly due to the jet veto and the presence of extra jets at NLO. The efficiency for the other selection cuts is very similar at LO and NLO.

Table 4: Higgs-boson selection cut efficiencies for the Wt process at LO and NLO simulated with MCFM (parton level) [10] and TopREX (LO and parton shower). Here a veto is applied to the p_t of the generated b and is set at 40 GeV. The cross section is given for the decay branching ratio $[W^+ \to e^-\nu][t \to e^-\nu\bar{b}]$.

| | MCFM | | | | TopREX |
| | LO | | NLO | | LO |
Selection cuts	$\sigma \times BR$ (fb)	rel. eff	$\sigma \times BR$ (fb)	rel. eff	rel. eff
No cuts	271		377		
2 lep, $|\eta| < 2$, $p_t > 20$ GeV	204	0.75±0.002	277	0.73±0.002	
$E_t^{miss} > 40$	148	0.73±0.002	209	0.75±0.003	0.75±0.001
$\phi_{\ell\ell} < 45$	20.8	0.14±0.002	34.4	0.16±0.002	0.17±0.001
5 GeV $< m_{\ell\ell} < 40$ GeV	10.6	0.51±0.01	15.6	0.45±0.008	0.50±0.005
Partonic jet veto, 40 GeV	1.55	0.15±0.01	1.12	0.07±0.006	0.16±0.005
30 GeV$< p_t^{\ell\,max} <$55 GeV	1.08	0.70±0.03	0.73	0.65±0.05	0.63±0.02
$p_t^{\ell\,min} >$25 GeV	0.73	0.68±0.04	0.49	0.67±0.05	0.67±0.02

The selection efficiency obtained with MCFM was then compared to a simulation done with TopREX where the parton shower was added. The cut efficiencies for TopREX are shown in the fifth column of Table 4. TopREX and MCFM lead to very similar results. Thus TopREX should lead to a good simulation of single resonant top production. To account for the difference in the jet veto efficiency between NLO and LO, the K-factor that will be used to approximate NLO cross sections is determined in the signal region and is 0.7. This also avoids double counting between double and single resonant top production since the two processes are separated in the signal region. After a jet veto requirement the diagrams that can be double counted bring a negligible contribution [9]. A theoretical uncertainty from scale variation and PDF uncertainty of about 20% can be expected on these numbers [13].

Experimentally, the jet veto is applied to reconstructed jets[8] and the jet energy does not correspond to an exact

---

[7] Previous attempts to remove these contributions have either relied on subtracting the double-resonant cross section [7] or on applying a mass window cut [8], both of which suffer from ambiguities related to the interference between the single- and double- resonant graphs.

[8] For this study, as before, the jets are reconstructed applying a cone algorithm to the generated stable particles.

value of the parton p_t. At Leading Order, requiring no parton with $p_t > 40$ GeV, has a similar efficiency to requiring no jets with $p_t > 30$ GeV. Thus a parton cut at 40 GeV will roughly correspond to a jet cut at 30 GeV. Figure 11 shows the selection efficiency for finding two leptons with $p_t > 20$GeV and vetoing all cone jets with $p_t > 30$ GeV as a function of the p_t of the b. In this case, 85% of the events have $p_t(b) < 40$ GeV and 94% have $p_t(b) < 60$ GeV.
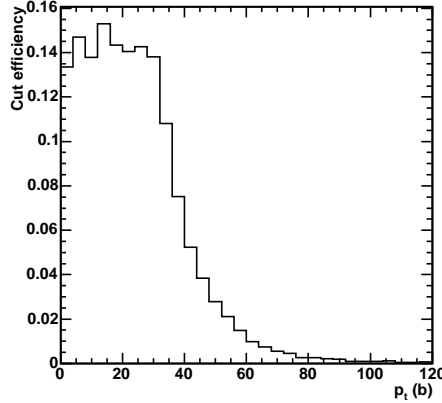

Figure 11: Cut efficiency as a function of the b transverse momentum, after requiring two isolated leptons with $p_t > 20$ GeV, $|\eta| < 2$ and no reconstructed cone jet with $p_t > 30$ GeV for a simulation using TopREX.

We propose thus to use TopREX for the generation of such process and then constant K-factors determined in the particular signal region. The theoretical error on the Wt cross section is estimated to be around 20% including PDF and scale variation.

4 $t\bar{t}$ normalization

The presence of two neutrinos in the final state of the decay $H \rightarrow W^+W^- \rightarrow \ell^+\nu\ell^-\bar{\nu}$ does not allow the reconstruction of a narrow mass peak. Moreover, the rejection needed to reduce the different background processes is very high. In the specific case of $t\bar{t}$ it is $\mathcal{O}(10^5)$. The precise understanding of the backgrounds is then the most critical issue concerning this Higgs-boson discovery channel. The most reliable approach to address this problem is to measure the different sources of background directly from the data. The commonly used method consists of selecting a signal-free phase space region (control region) where a given background process is enhanced. The contribution of that background in the signal region is then extrapolated from the measured number of events in the control region. This procedure relies on the following relation:

$$N_{\text{signal\_reg}} = \frac{N_{\text{signal\_reg}}^{\text{MonteCarlo}}}{N_{\text{control\_reg}}^{\text{MonteCarlo}}} N_{\text{control\_reg}} = \frac{\sigma_{\text{signal\_reg}} \cdot \epsilon_{\text{signal\_reg}}}{\sigma_{\text{control\_reg}} \cdot \epsilon_{\text{control\_reg}}} N_{\text{control\_reg}} \tag{1}$$

where $N_{\text{signal\_reg}}^{\text{MonteCarlo}}$ and $N_{\text{control\_reg}}^{\text{MonteCarlo}}$ are the numbers of events predicted by the Monte Carlo simulation in the signal and control region. Each of these two numbers can be expressed as a product of the theoretical cross section in that phase space area, $\sigma_{\text{signal\_reg}}$ and $\sigma_{\text{control\_reg}}$, and the experimental efficiency of reconstructing events in the same region, ϵ_{signal} and $\epsilon_{\text{control\_reg}}$[9]. This allows to better point out the different sources of systematic uncertainties. In particular, the theoretical predictions enter the procedure only via the ratio $\sigma_{\text{signal\_reg}}/\sigma_{\text{control\_reg}}$, leading to reduced scale dependency and thus to reduced theoretical uncertainties.

The theoretical issues concerning the $t\bar{t}$ normalization are discussed in [16], following the work done in the 2003 Les Houches Workshop. The goal of this note is not to review the theoretical basis of the method, but to provide a reliable description of the experimental aspects and to discuss the related systematic uncertainties by means of a full detector simulation.

The characteristics that the control region should have, in order to keep the systematic uncertainties as low as possible, are the following:

---

[9] The experimental uncertainties could modify the boundaries defining the phase space where the cross section is calculated theoretically. This is the case in particular when the selections involve jets. The efficiencies in relation (1) are assumed to account also for this effect.

- Theoretical calculations should be reliable in that phase space area

- The contamination from other processes should be small

- The selections for the signal and control phase space regions should be as similar as possible

To match the last requirement listed above, both control regions will be defined by the same selections on the leptons as for the signal region. In order to estimate the contribution of the $t\bar{t}$ process in the signal region, we exploit the two additional high E_t jets coming from the b quark fragmentation. Two procedures are proposed to enhance the $t\bar{t}$ contribution: the b-tagging of the two jets and hte requirement of the E_t of the jets to be above a certain threshold. As all selection criteria are unchanged, only the systematics concerning the b-tagging, the jet reconstruction and the vetoing efficiencies have to be estimated.

The contribution from other processes into the control regions, including the signal itself, will be treated as an additional systematic uncertainty, if it represents a sizable fraction of the expected number of events.

As discussed in the previous section, the theoretical prediction for $gb \rightarrow Wt$ at NLO is reliable only for the "$2\ell+b$" final state, i.e. when a veto is applied on all jets but the one from the top. This implies that we can not measure the Wt background by means of the same strategies as for $t\bar{t}$, since it does not match the first requirement listed above. The definition of an additional control region for Wt would require a dedicated study with this process treated as the signal. Provided that the contribution of Wt in the signal region is smaller than the $t\bar{t}$ one and that a NLO prediction for the cross section in that phase space area is available, the strategy for the evaluation of the Wt background from the data is not addressed in this note.

The cuts used to define the signal region together with the corresponding number of events expected for 1 fb^{-1} for the fully simulated signal (for a Higgs-boson mass of 165 GeV), $t\bar{t}$ and Wt are summarized in Table 5. They are slightly different from the cuts applied in Table 2, as these criteria are adjusted to a complete detector simulation.

In this full simulation context the jet reconstruction-algorithm is based on an iterative procedure applied on energy deposits in the calorimeter (ECAL+HCAL) towers within a 0.5 cone. The E_t threshold for the tower seeding the algorithm is set to 1 GeV, whereas the E_t and E thresholds for a tower to be included in the jet are respectively 0.5 and 0.8 GeV. The jets energy is not calibrated.

The jet veto is applied to the events with at least one jet with $E_t > 20$ GeV within $|\eta| = 2.5$. Moreover if a jet with E_t in the range $[15, 20]$ GeV with $\alpha > 0.2$ is found, the event is rejected. α is a parameter that quantifies the track content of a jet. It is defined by the ratio of the sum of the p_t of all tracks inside the jet over the transverse jet energy deposed in the calorimeter[10] [14].

Table 5: The expected number of events for a luminosity of 1 fb^{-1} for the signal with a Higgs-boson mass of 165 GeV and the $t\bar{t}$ and Wt background. The relative efficiency with respect to the previous cut is given inside the brackets in percent.

	H $\rightarrow$ WW $m_H = 165$ GeV		$t\bar{t}$		Wt	
$\sigma \times$ BR(e, μ, τ) [fb]	2360		86200		3400	
Trigger L1+HLT	1390	0.59$\pm$0.002	57380	0.67$\pm$0.001	2320	0.68$\pm$0.001
2 lep, $|\eta| < 2$, $p_t > 20$ GeV $\sigma_{IP} > 3$, $|\Delta z_{lep}| < 0.2$ cm	393	0.28$\pm$0.003	15700	0.27$\pm$0.002	676	0.29$\pm$0.002
$E_t^{miss} > 50$ GeV	274	0.70$\pm$0.005	9332	0.59$\pm$0.002	391	0.58$\pm$0.003
$\phi_{\ell\ell} < 45$	158	0.58$\pm$0.006	1649	0.18$\pm$0.002	65	0.17$\pm$0.003
12 GeV $< m_{\ell\ell} < 40$ GeV	119	0.75$\pm$0.007	661	0.40$\pm$0.006	28	0.43$\pm$0.009
30 GeV$< p_t^{\ell\,max} <$55 GeV	88	0.74$\pm$0.008	304	0.46$\pm$0.009	13	0.46$\pm$0.01
$p_t^{\ell\,min} >$25 GeV	75	0.86$\pm$0.01	220	0.74$\pm$0.01	9.2	0.71$\pm$0.02
Jet veto	46	0.63$\pm$0.01	9.8	0.044$\pm$0.007	1.4	0.15$\pm$0.02

---

[10] In order be included in the alpha determination, a track: has to be 'inside' the jet, $\Delta R_{track-jet} < 0.5$, has to come from the event vertex, $|z_{trk} - z_{vtx}| <$0.4 cm, should have more than 5 hits and $p_t > 2$ GeV.

Normalization with b-tagging jets

The presence of two b-tagged jets is a striking evidence for $t\bar{t}$ events. The algorithm used to discriminate whether a jet is originated from a b quark is based on the impact parameters of charged tracks associated to the jet [15]. The parameter that characterizes the efficiency and the mistagging rate of the algorithm is the impact parameter significance of a minimum number of tracks associated to the jet, σ_{IP}. In this study a jet is tagged as a b-jet if its measured E_t is greater then 20 GeV and if there are at least 2 tracks whose σ_{IP} is higher than a given threshold[11]. A compromise is needed between a small statistical uncertainty, which means to have a high efficiency in selecting $t\bar{t}$ events, and limiting the systematic uncertainties due to the contamination from other processes, which requires keeping the mistagging rate as low as possible.

In order to find out the most suitable working point, the efficiency, the purity and the mistagging rate have been studied as a function of σ_{IP}. The results are shown in Figure 12. The solid line in left plot of Figure 12 represents the efficiency of tagging at least 1 jet as coming from a b-quark when actually 2 b's are present within $|\eta| < 2.5$, the left plot refers to tagging at least 2 jets.

The dashed line represents the fraction of b-tagged jets which match the b-parton direction with a precision of $\Delta R < 0.5$. The left plot shows the matching efficiency for one b-tagged jet, while on the right plot the direction of two b-tagged jets must match those of the corresponding 2 b-quarks.
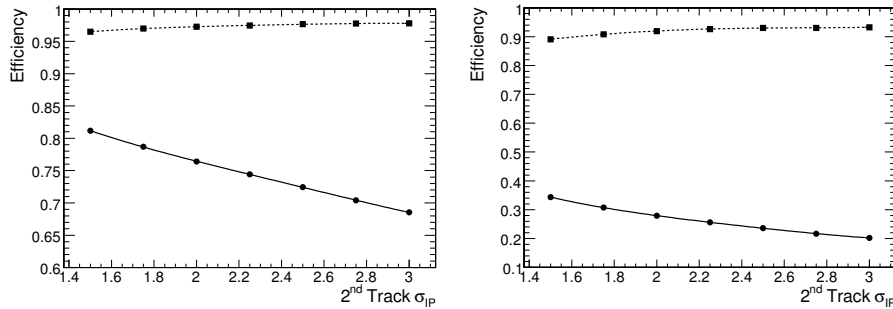

Figure 12: Jet b-tagging efficiency (solid line) and matching efficiency (dashed line). On the left plot the efficiency of b-tagging and matching with a b parton at least one jet out of two is shown. On the right plot the efficiency of b-tagging two jets is shown.

To quantify the mistagging rate we select events without bottom quarks out of a sample of Drell-Yan production with muons in the final state. The mistagging rate is calculated from the ratio between the number of b-tagged jets and the total number of jet with $E_t > 20$ GeV. The results are shown in Figure 13.
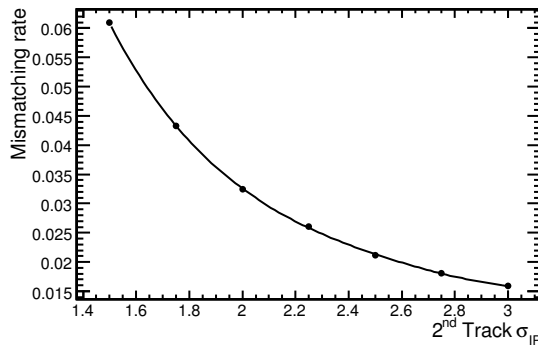

Figure 13: Ratio between the number of b-tagged jets and the total number of jets with $E_t > 20$ GeV as a function of the discriminator value.

Finally the number of events in the control region for 10 fb^{-1} as a function of σ_{IP} is computed. Table 6 summarizes the results for $t\bar{t}$, Wt and the signal in the case of 2μ, 2e and eμ final states. In addition to the request of two b-tagged jets, all cuts defining the signal region from 1 to 7 in Table 5, but the jet veto, are applied.

---

[11] The number of tracks whose σ_{IP} has to be higher then the cut could be varied as well. In this study the default value of 2 tracks has been used.

Table 6: Number of $t\bar{t}$, signal and Wt events expected for 10 fb^{-1} in the control region defined by requiring two b-tagged jets, as a function of σ_{IP}. Results are shown for each possible leptonic final state. The statistical uncertainty on $t\bar{t}$ events due to Monte Carlo statistics ranges between 10 and 20%.

σ_{IP}	2μ			$2e$			$e\mu$		
	$t\bar{t}$	Signal	Wt	$t\bar{t}$	Signal	Wt	$t\bar{t}$	Signal	Wt
1.5	218	1	2	128	< 1	< 1	294	2	4
1.75	211	1	2	118	< 1	< 1	266	1	3
2	194	< 1	1	107	< 1	< 1	245	1	2
2.25	183	< 1	1	86	< 1	< 1	232	1	2
2.5	173	< 1	1	69	< 1	< 1	218	< 1	1
2.75	166	< 1	1	62	< 1	< 1	211	< 1	1
3	152	< 1	< 1	59	< 1	< 1	194	< 1	1

In the following the cut $\sigma_{IP} > 2$ is chosen, corresponding to a b-tagging efficiency for two tags is $\mathcal{O}(30\%)$, while the mistagging rate is $\mathcal{O}(3\%)$.

Not all the processes with $2\ell + 2b + E_t^{miss}$ as the final state have been fully simulated for this analysis. Nevertheless general considerations and fast Monte Carlo checks can be used to exclude other relevant sources of backgrounds. The more natural concurrent process is $W^+W^- \rightarrow 2\ell + b\bar{b}$ which is anyway α_{weak}^2 suppressed with respect to $t\bar{t}$. Its cross section is indeed expected to be smaller than 1 pb. Assuming the same efficiency for the kinematic selections as for the $W^+W^- \rightarrow 2\ell$, i.e. $\mathcal{O}(10^{-3})$, less than 10 events are expected for 10 fb^{-1} in the control region even without applying the double-b tagging efficiency. In the case of same flavour leptons in the final state, $\gamma^*/Z^* \rightarrow 2\ell + b\bar{b}$ (the vector boson mass being away from the Z peak, i.e. $m_{\ell\ell} < 40$ GeV) could also contribute. Although not having prompt neutrinos producing a high value of E_t^{miss}, it is safe to check that the tail in the measured distribution is not wide enough to promote this process to a relevant background. Figure 14 shows the E_t^{miss} spectrum for fully simulated $\gamma^*/Z^* \rightarrow 2\mu + 2b$ events, with the 2 b-jets with $E_t > 20$ GeV. Less than 1 % of the events satisfy $E_t^{miss} > 50$ GeV, the cut applied for the signal selection.
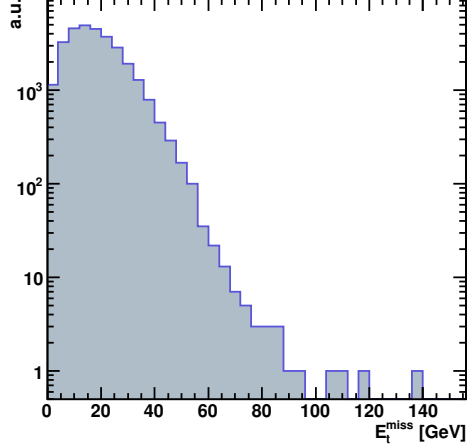

Figure 14: E_t^{miss} spectrum for $\gamma^*/Z^* \rightarrow 2\mu + 2j$ events

In order to estimate the contribution of $pp \rightarrow \gamma^*/Z^* \rightarrow 2\ell + b\bar{b}$ to the actual control region, a parton level sample has been generated using the MadGraph Monte Carlo [11]. About 200 events are expected for 10 fb^{-1} after applying the same kinematic selections, except for the E_t^{miss} cut. The latter cut and the double b-tagging requirement applied to fully simulated events provide a reduction larger than 99%, enough to safely exclude this background.

Normalization with two high E_t jets

Although very powerful, the method proposed above for $t\bar{t}$ estimation from data relies entirely on jet b-tagging: a sophisticated procedure both from the hardware and the algorithmic point of view. The performance of the vertex and tracking detectors will need to be well understood and verified against simple event samples before being

regarded as trustworthy enough to be exploited for new physics analysis. Given the fact that, if the Higgs boson has a mass between 150 and 170 GeV, a signal could already be seen with a very low luminosity, it is then important to have alternative methods to estimate the $t\bar{t}$ background from data.

Each of the two b's in the $t\bar{t}$ final state come from a 175 GeV central object; their E_t spectra are then rather hard. An alternative method to define a $t\bar{t}$ control region is then simply to require, in addition to the signal kinematic cuts, two hard jets in the detector.

Analogously to the b-tagging jets based normalization, Drell Yan events can be a dangerous background. In this case the general $2\ell + 2j$ final state has a much higher cross section with respect to the $2\ell + 2b$ one. A Monte Carlo level analysis has been performed, leading to the result that, after applying the $\mathcal{O}(10^{-2})$ reduction due to the E_t^{miss} cut, the contribution of this process in such control region can not be neglected. To reduce this additional background, only the $e\mu$ final state will be considered. The same flavour final state then will have to rely on the double b-tagged jets normalization procedure.

Table 7 shows the number of events expected for $t\bar{t}$, Wt and the signal in 10 fb^{-1} as a function of the E_t thresholds applied to the jets are shown. All cuts defining the signal region, from 1 to 7 in Table 5, but the jet veto are applied. In the following, the jet E_t thresholds are chosen as 50 and 30 GeV.

Table 7: Number of $t\bar{t}$, signal and Wt events expected for 10 fb^{-1} in the control region defined by requiring two hard jets, as a function of the $t\bar{t}$ thresholds. Results are shown only for the $e\mu$ final state. The statistical error on $t\bar{t}$ events due to Monte Carlo statistics is less than 10%. For the chosen E_t thresholds, 50 and 30 GeV, the statistical uncertainty on the predicted number of signal and Wt events are respectively 20 and 30%.

$t\bar{t}$						
E_t thr. 1 [GeV] / E_t thr. 2 [GeV]	35	40	45	50	55	60
25	601	556	511	453	391	346
30	511	487	449	411	356	325
35	432	418	397	373	321	294
40		325	318	301	266	245
45			256	245	232	214

Signal (M$_H$=165 GeV)						
E_t thr. 1 [GeV] / E_t thr. 2 [GeV]	35	40	45	50	55	60
25	17	15	14	12	11	10
30	14	13	12	11	10	9
35	11	10	9	8	8	7
40		8	8	7	7	6
45			6	5	5	4

Wt						
E_t thr. 1 [GeV] / E_t thr. 2 [GeV]	35	40	45	50	55	60
25	11	10	9	8	7	7
30	8	7	6	6	5	4
35	6	5	4	4	4	3
40		4	3	3	3	2
45			2	2	2	1

A background process not considered in the full simulation analysis is $W^+W^- \rightarrow \mu\nu_\mu + e\nu_e + 2j$. In order to compute the contamination due to this process, a generator-level study based on events produced by the MadGraph Monte Carlo was performed. The cross section, after geometrical acceptance cuts, is 0.4 pb, whereas the signal efficiency is smaller than $5 \cdot 10^{-4}$ (with a statistical error of $\sim 8\%$). The contribution of this background can then be assumed to be at most of the same order as the signal.

If one jet is misidentified as an electron, the $W^\pm \rightarrow \mu\nu_\mu + 3j$ process could also provide the same final state topology. The probability of electron misidentification is estimated to be $\mathcal{O}(10^{-4})$[12]. The cross section of this

process is about 200 pb after the acceptance cuts. The kinematic selection efficiency is estimated to be of the order of $\mathcal{O}(10^{-4})$ and therefore this source of contamination is negligible.

In Table 8 the results concerning the number of $t\bar{t}$ events expected for 10 fb^{-1} in the signal and control regions are summarized.

Table 8: Number of $t\bar{t}$ events expected for 10 fb^{-1} in the signal and control regions. Both control region are defined by all the cuts listed in Table 5 but the jet veto. The "b-tagging" control region requires the presence of two jets with a b-tag discriminator value greater then 2 whereas the "hard jets" control region includes events with two jets with E_t respectively greater then 50 and 30 GeV. The statistical uncertainties due to Monte Carlo samples statistics are shown in parentheses.

	2μ	2e	eμ
Signal region	33 (± 9)	22 (± 8)	44 (± 11)
"b-tagging" control region	194 (± 25)	107 (± 19)	245 (± 29)
"hard jets" control region	-	-	411 (± 39)

5 Normalization uncertainties

5.1 Systematics uncertainties

Our proposed procedures to estimate the number of $t\bar{t}$ events in the signal phase space region exploits relation (1). In order to compute the systematic uncertainties on the final result we consider separately each term of the formula.

- **Theoretical uncertainty.**

  Taking the ratio of the $t\bar{t}$ cross sections in the signal and control region avoids much of the theoretical systematic uncertainties. In Ref. [16] the theoretical uncertainty on the ratio $\sigma_{\text{signal\_reg}}/\sigma_{\text{control\_reg}}$ has been studied at parton level with LO precision by varying the renormalization and factorization scale. The error has been estimated to range between 3% to 10%, mostly due to the choice of the PDF.

  Section 2 has shown that the shapes of the distributions involved in the normalization procedure, i.e. the E_t spectra of the jets and the jets multiplicity are not affected by higher orders contributions. However, the comparison of different showering models shows some discrepancies either in the jets multiplicity and the jets E_t spectra, introducing a further uncertainty in addition to those due to the PDF set. The effect of these uncertainties on the proposed normalization procedure have not been studied in this analysis. It is expected that the Monte Carlo predictions concerning $t\bar{t}$ topologies and kinematics will be intensively compared and tuned directly with the copious data at the LHC. This will help in reducing much of our present theoretical uncertainty due to the lack of experimental insight on the 14 TeV phenomenology[13].

  In the following we will assume the theoretical uncertainty on the normalization procedure to be 10% as suggested in Ref. [16], even though this could be an optimistic estimation.

- **Jet Energy Scale uncertainty.**

  The Jet Energy Scale (JES) uncertainty is particularly important since it affects in opposite ways the signal region, defined by vetoing the jets, and the control region where the presence of two jets is required. To take into account the anticorrelation of $\epsilon_{\text{signal\_reg}}$ and $\epsilon_{\text{control\_reg}}$, we estimate the effect of the JES uncertainty directly on their ratio by rescaling the measured jet four momentum by a fractional uncertainty: $P'_{\text{jet}} = (1 + \lambda)P_{\text{jet}}$.

  Figure 15 shows the relative variation of $\frac{\epsilon_{\text{signal\_reg}}}{\epsilon_{\text{control\_reg}}}$ for various values of λ[14]. The triangles represent the control region defined by requiring two jets with E_t higher than 50 and 30 GeV respectively, whereas the squares stand for the control region defined by requiring two jets with $\sigma_{\text{IP}} > 2$. In the latter case, the ratio $\epsilon_{\text{signal\_reg}}/\epsilon_{\text{control\_reg}}$ is less sensitive to the JES uncertainty as the E_t threshold for the b-jets candidates is 20 GeV and the few $t\bar{t}$ events have b-tagged jets with E_t close to that threshold.

---

[12] The muon misidentification rate is expected to be at least one order of magnitude smaller

[13] How much the theoretical uncertainty will be once the LHC data will be available is something that exceeds the scope of this study, being the subject of a wider and more general analysis.

[14] The dependency of the JES uncertainty from the jet E_t is taken into account by dividing λ by 2 for jets above 50 GeV.

The JES uncertainty for the first 1 fb^{-1} of data is foreseen to be 10% for jets with $E_t \sim 20$ GeV and 5% for jets with $E_t > 50$ GeV, using a calibration based on $t\bar{t}$ events. These uncertainties are expected to be reduced by half with 10 fb^{-1} of integrated luminosity. For this integrated luminosity, the corresponding relative variation of $\epsilon_{\text{signal\_reg}}/\epsilon_{\text{control\_reg}}$ is $\sim 8\%$ for the control region defined by b-tagging and $\sim 10\%$ for the control region defined by high-E_t jets.
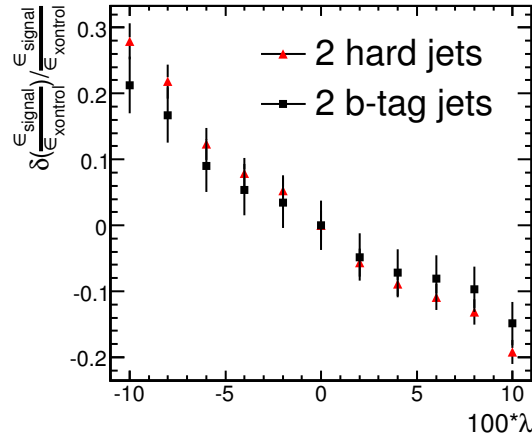

Figure 15: Relative variation of $\frac{\epsilon_{\text{signal\_reg}}}{\epsilon_{\text{control\_reg}}}$ as a function the jet momentum rescaling factor (λ). The triangles represent the control region defined by two hard jets whereas the squares correspond to the two b-tagged jets phase space area.

- **α criterion uncertainty.**

  To prevent the contamination from fakes when vetoing jets down to a raw transverse energy of 15 GeV, it is useful to cut on the track content of the jets. For jets with E_t ranging from 15 to 20 GeV, as explained in section 4, the α criterion is then exploited.

  To estimate the systematic uncertainty due to this criterion, the cut on α has been varied from 0.15 to 0.25. Moreover different values of the minimum p_t for a track to be included in the sum have been tried, from 2 to 3 GeV. These changes imply a variation of $\epsilon_{\text{signal\_reg}}$ of about 4%.

- **b-tagging uncertainty.**

  The precision with which the b-tagging efficiency will be known is expected to be $\pm 11\%$ for 1 fb^{-1} integrated luminosity and it is foreseen to improve to $\pm 7\%$ with 10 fb^{-1} [17]. These values are used for the uncertainty on $\epsilon_{\text{control\_reg}}$ if the control region is defined by requiring two b-tagged jets.

- **Uncertainties on $N_{\text{control\_reg}}$.**

  The selection criteria used to identify the control region identify almost entirely $t\bar{t}$ events. In the worst case, i.e. when the control region is defined by two high E_t jets, the fraction of events coming form other processes is smaller than 4%. Provided that this fraction is small, it is safe to simply neglect this source of systematic error.

The experimental systematics involved in the $t\bar{t}$ normalization procedure are summarized in Table 9. For an integrated luminosity of 10 fb^{-1} these uncertainties are about 11% for both control regions. Including the assumed 10% theoretical uncertainty this uncertainty becomes 15%.

5.2 Statistical uncertainties

The statistical precision on the estimation of the $t\bar{t}$ background in the signal region depends on the expected number of $t\bar{t}$ events in the control region. Figure 16 shows the Poisson errors on $N_{\text{control\_reg}}$ as a function of the integrated luminosity. In the left plot the curves represent the control region defined by requiring two jets with a b-tagging discriminator value higher then 2. whereas the left plot concerns the control region defined by requiring two jets with E_t higher then 50 and 30 GeV.

Compared at the same luminosity, the error due to systematic uncertainties dominates with respect to the statistical errors for both the proposed normalization procedures.

Table 9: Summary of the different experimental systematics involved in the $t\bar{t}$ normalization procedure. The total uncetainties are calculated by adding quadratically each single contribution. Results are shown for an integrated luminosity of 10 fb^{-1}.

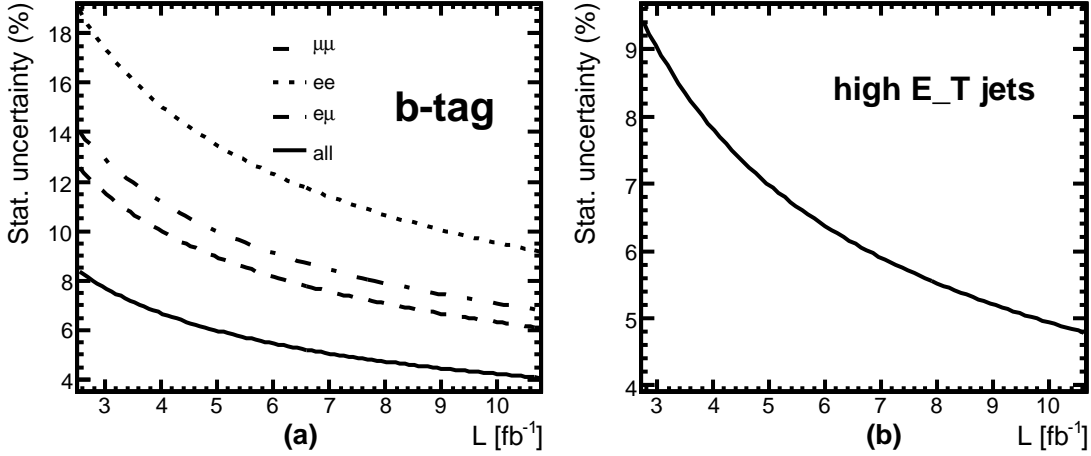| Uncertainty	"b-tagging" control region	"hard jets" control region
JES	8%	10%
$b-$tagging	7%	-
α criterion	4%	4%
$N_{control\_reg}$	negligible	negligible
Total	11.4%	10.8%

Figure 16: Poisson statistical uncertainty on the number of $t\bar{t}$ as a function of the integrated luminosity if a.) b-tagging or b.) two high-E_t jets are used to identify the control region. In b.) only the eμ final state is considered.

6   Conclusions

The $t\bar{t}$ production at the LHC is one of the main backgrounds for the H $\rightarrow$ WW $\rightarrow$ $\ell\nu\ell\nu$ signal search.

Single-resonant top production was studied comparing the MCFM and TopReX Monte Carlo programs. Its simulation and normalization of the $t\bar{t}$ background were studied in detail . NLO corrections to the Wt background can be studied independently of the double resonant $t\bar{t}$ process in the signal region, scaling the LO cross section with a K-factor of 0.7.

Double resonant $t\bar{t}$ production was studied comparing four different Monte Carlos. NLO corrections to the $t\bar{t}$ background can be taken into account by scaling the LO results to the corresponding NLO cross section of 840 pb, as the shape of the different variables used for the Higgs-signal selection are very similar at LO and NLO. The differences observed between the different Monte Carlo generators mainly originate from the modeling of showers and the inclusion of spin correlation. The difference due to the showering model is around 20% while the spin correlations lead to a systematic uncertainty of 10%. These uncertainties make it important to estimate the $t\bar{t}$ background from data.

Two methods were developed to normalize the $t\bar{t}$ background, the first based on the tagging of the two jets as originating from b quarks and the other simply requiring two high-E_t jets. The experimental systematics of these normalization methods are estimated to be about 11%. Including statistical uncertainties and the estimates of theoretical uncertainties from ef.[NikolasttNorm], both procedures lead to a total uncertainty of 16% with an integrated luminosity of 10 fb^{-1}.

7   Acknowledgments

References

[1] M. Dittmar and H. K. Dreiner, "How to find a Higgs boson with a mass between 155 GeV to 180 GeV at the LHC", Phys. Rev. D **55** (1997) 167 [arXiv:hep-ph/9608317].

[2] T. Sjostrand, L. Lonnblad, S. Mrenna and P. Skands, "PYTHIA 6.3: Physics and manual", [arXiv:hep-ph/0308153].

[3] S.R. Slabospitsky, L. Sonnenschein, Comput. Phys. Commun. **148** (2002) 87, [arXiv:hep-ph/0201292]

[4] HERWIG 6.5, G. Corcella, I.G. Knowles, G. Marchesini, S. Moretti, K. Odagiri, P. Richardson, M.H. Seymour and B.R. Webber, JHEP 0101 (2001) 010 [hep-ph/0011363]; hep-ph/0210213.

[5] S. Frixione and B. R. Webber, "Matching NLO QCD computations and parton shower simulations", JHEP **0206** (2002) 029 [arXiv:hep-ph/0204244]
S. Frixione, P. Nason and B. R. Webber, "Matching NLO QCD and parton showers in heavy flavour production", JHEP **0308** (2003) 007 [arXiv:hep-ph/0305252].

[6] G. Davatz, G. Dissertori, M. Dittmar, M. Grazzini and F. Pauss, "Effective K-factors for g g → H → W W → l nu l nu at the LHC", JHEP **0405** (2004) 009 [arXiv:hep-ph/0402218].

[7] T. M. P. Tait, Phys. Rev. D **61** (2000) 034001 [arXiv:hep-ph/9909352].

[8] A. Belyaev and E. Boos, Phys. Rev. D **63** (2001) 034012 [arXiv:hep-ph/0003260].

[9] J. Campbell and F. Tramontano, "Next-to-leading order corrections to W t production and decay", [arXiv:hep-ph/0506289].

[10] J. Campbell and K. Ellis, "Monte Carlo for FeMtobarn processes", http://mcfm.fnal.gov/

[11] F. Maltoni and T. Stelzer, JHEP **0302** (2003) 027 [arXiv:hep-ph/0208156].

[12] The CMS Collaboration, 'The Trigger and Data Acquisition project, Volume II', CERN/LHCC 2002-26, CMS TDR 6.2, 15 December 2002

[13] J. Campbell, private communication.

[14] Following an idea developped by N. Ilina, V. Gavrilov and A. Krokhotin and implemented like in: **CMS NOTE-2006/047**, G. Davatz, M. Dittmar, A.-S. Giolo-Nicollerat, *Standard Model Higgs Discovery Potential of CMS in the* H → WW → $\ell\nu\ell\nu$ *Channel*

[15] **CMS NOTE-2002/046**, F. Palla and G. Segneri, *Lifetime Based b-tagging with CMS*

[16] N. Kauer "Top Background Extrapolation for H → WW Searches at the LHC", Phys. Rev. D **70** (2004) 014020 [arXiv:hep-ph/0404045].

[17] **CMS NOTE-2006/013** J. D'Hondt, J. Heyninck, S. Lowette and P. Vanlear, *Offline Calibration of b-Jet Identification Efficiency*